Electronic Supplementary Material (ESI) for Environmental Science: Water Research & Technology.
This journal is © The Royal Society of Chemistry 2016

Supplementary Information for:

Trihalomethane, Dihaloacetonitrile, and Total *N*-nitrosamine Precursor Adsorption by Carbon Nanotubes: The Importance of Surface Oxides and Pore Volume

AUTHORS:

Erin M. Needham [a], Shelby M. Sidney [a], Justin R. Chimka [b], and Julian L. Fairey [a,]*

AUTHOR AFFILIATIONS:

[a] Department of Civil Engineering, University of Arkansas, Fayetteville, AR 72701, USA

[b] Department of Industrial Engineering, University of Arkansas, Fayetteville, AR 72701, USA

[*] Corresponding author:

Julian L. Fairey, Ph.D., P.E.

Associate Professor, Department of Civil Engineering

Address: 4190 Bell Engineering Center, Fayetteville, AR 72701, USA

Phone: (479) 575-4023

Fax: (479) 575-7168

Email: julianf@uark.edu

Supplementary Information contains: Methods; PARAFAC Analysis; Carbon Spectra Deconvolutions; Model Verification and Permutations; Modeling CNT Wall Type; Removal of PARAFAC Components; PARAFAC Component Correlations; UV_{254} as a DBP Precursor Surrogate; References; 21 pages, 7 tables and 9 figures

List of Supplementary Information

Methods

Dissolved organic carbon was measured for each filtered sample using a GE 5310C TOC analyzer. Anion concentrations were measured for both BL-RAW and WS-EFF raw waters using a Metrohm 850 Ion Chromatograph with conductivity and UV detectors. Fluorescence EEMs were collected using a dual monochromator fluorescence detector (Agilent Technologies, Model G1321A). Wavelengths used were 250 to 400 nm for excitation and 270 to 600 nm for emission, both in 1 nm increments. A five-point standard curve of quinine sulfate in 0.1 M sulfuric acid was used due to its distinct response at excitation and emission wavelengths of 350 and 450 nm, respectively, and intensity measurements of all spectra were reported in quinine sulfate equivalents.[1] Absorbance scans were used to correct for inner-filter effects as suggested by McKnight et al.[2] and the MATLAB program *Cleanscan*[3] was used to correct EEMs for Raleigh and Raman scattering. Values of fluorescence intensity at excitation and emission wavelengths of 345 nm and 425 nm, respectively, are strongly correlated with TTHM precursors[4] and are shown in Table S1 for both BL-RAW and WS-EFF. Two models were developed using parallel factor (PARAFAC) analysis on arrays of EEMs for each water type to reveal components with distinct excitation-emission signatures and their maximum intensities, F_{MAX}.[5]

Disinfection by-product formation potential (DBPFP) of the samples was measured using the procedure detailed in Do et al.[4] Samples were warmed to room temperature, amended with 20 mM sodium bicarbonate, and adjusted to pH 7.0 using NaOH and/or HCl. Pre-formed 14 $g \cdot L^{-1}$ as Cl_2 stock monochloramine solution was prepared immediately before chloramination as detailed previously. The stock total

chlorine and monochloramine concentrations were measured on a representative sample volume, following 4,000-6,000 times dilution with Milli-Q water, using Hach powder pillows with a UV-Vis 2450 spectrophotometer (Shimadzu) at wavelengths of 655- and 552 nm, respectively. Samples were dosed with pre-formed monochloramine at 300 $mg \cdot L^{-1}$ as Cl_2 and stored headspace-free in 1-L chlorine demand free amber glass bottles for 7 days in the dark at room temperature (25 ºC ± 2 ºC). Following the hold time, the monochloramine and total chlorine residuals were measured and quenched with 20.1 g of a salt mixture (mass ratio of 0.9 g ascorbic acid ($C_6H_8O_6$): 1 g KH_2PO_4: 39 g Na_2HPO_4) added to each 1 L sample to halt DBP formation reactions as recommended by Kristiana et al.[6] Total trihalomethanes (TTHMs) and dihaloacetonitriles (DHANs) in the West Side wastewater treatment plant effluent (WS-EFF) samples were quantified by GC-ECD using a 9-point standard curve that ranged from 1- to 100 $\mu g \cdot L^{-1}$. Similarly, TTHMs and DHANs in the Beaver Lake raw water (BL-RAW) samples were analyzed using a 12-point standard curve that ranged from 0.1- to 100 $\mu g \cdot L^{-1}$. Blanks and check standards were run after every group of six samples.

The pH point of zero charge of the carbon nanotubes (CNTs) was not measured because a stable suspension could not be achieved without CNT modification. Sonication of CNTs in pure water was attempted despite the high probability of damage to the CNT structure,[7] but failed to produce the stable suspension necessary for zeta potential measurements.

97 **PARAFAC Analysis**

98 EEMs were analyzed by PARAFAC to further characterize the dissolved organic
99 matter and help generalize the precursor surrogate findings. Given the differences in the
100 water types, separate PARAFAC models were used for BL-RAW and WS-EFF samples,
101 each originally consisting of 57 EEMs. Two outliers were removed from the BL-RAW
102 data set while no outliers were found in WS-EFF samples. Split-half analyses showed
103 that BL-RAW samples could be adequately described by a two- or four-component
104 model and the WS-EFF samples could be described by a two- or three-component model.
105 Models with the greatest number of components (i.e., four components for BL-RAW and
106 three components for WS-EFF) were chosen to explain the data because they had the
107 smallest sum of squared errors (Figure S8).

108 **XPS Data Analysis**

109 Binding energy scales were charge corrected using a C1s peak position of 284.4
110 eV.[8, 9] C1s peaks were deconvoluted with a Gaussian-Lorentzian mix function, allowed to
111 range from 70-80% Gaussian distribution, and a Shirley background subtraction.[9, 10] An
112 asymmetry parameter of 0.19 was applied to the peak representing carbon-carbon bonds;[8]
113 other bonds assigned were alcohols (C-O), carbonyls (C=O), and carboxyls (COO) with
114 an additional peak fitted to the shake-up features satellite located in the higher binding
115 energy region. Peak locations chosen for the carbon spectra deconvolutions were set as
116 allowable ranges based on ranges found in the literature. Actual peak locations were
117 allowed to vary within the set range in order to achieve the best fit determined by the chi-
118 squared value of the model. The assymetric carbon peak representing all types of carbon-
119 carbon bonding was set to 284.38-285.50 eV.[8, 10-13] Locations of various types of carbon-

120 oxygen bonds are as follows: alcohol at 286.00-287.53 eV, carbonyl at 286.45-288.03
121 eV, and carboxyl at 288.39-289.55 eV.[8, 9, 11-15] Shake-up features associated with π-π*
122 transitions were fitted at 289.00-291.60 eV.[11] Each individual peak was allowed to vary
123 from 70- to 80% Gaussian distribution in order to find the best fit.[9, 10, 16]

124 **Model Verification and Permutations**

125 Results in Table 2 are based on reasonable assumptions with respect to a normal
126 distribution of residuals and constant error variance. The results of the Wilk-Shapiro
127 test[17] for TTHM ($p = 0.788$), DHAN ($p = 0.066$) and TONO ($p = 0.339$) were all greater
128 than $p = 0.05$; we therefore fail to reject a normal distribution of residuals.

129 Further investigation of the relationships between physical and chemical
130 characteristics of the nine CNT types through simple linear regressions revealed strong
131 correlations between percent alcohol groups and S_{BET} ($R^2 = 0.95$) and CPV ($R^2 = 0.90$).
132 Multiple linear regression models of surface oxide groups and physical characteristics
133 showed that alcohol groups were significant to S_{BET} and CPV when controlling for
134 carbonyl and carboxyl groups. These findings show that multicollinearity of alcohol
135 groups and physical properties results in variance inflation factors ($VIF = (1 - R^2)^{-1}$,
136 where R^2 is relevant to a multiple linear regression model of one independent variable
137 versus the other independent variables) greater than ten, which could make it impossible
138 to observe otherwise significant independent variables in models of DBP ratio. Of the
139 physical and chemical characteristics, carboxyl groups suffer least from variance inflation
140 ($VIF = 1.27$), and it is possible that this variable serves as a surrogate for significance of
141 physical characteristics. To further study possible significance of alcohol groups in the
142 face of multicollinearity, the carbonyl groups variable, which was insignificant in all

143 models, was deleted from models of TTHM and DHAN Ratios. This deletion revealed
144 negative significance of alcohol groups to DHAN ratio, indicating that an increase in
145 alcohol groups improved removal of DHAN precursors.

146 As further evidence of multicollinearity, linear regression between S_{BET} and CPV
147 variables also results in a very strong correlation (R^2 = 0.97). However, in the
148 multivariate analysis including both physical variables, only CPV was significant to
149 changes in DBPFP Ratio when controlling for surface area. The same cannot be said of
150 S_{BET} when controlling for CPV. As the multivariate model is capable of providing a more
151 comprehensive assessment of the significance of variables than simple linear regression
152 of variable pairs, it is reasonable to conclude that CPV is a more relevant variable to
153 discuss than S_{BET} in terms of relationships to chemical characteristics and DBPFP Ratio.
154 Nevertheless, Figure S4 shows the linear regressions for the wavelength pair associated
155 with the maximum R^2 value for TTHM ($I_{369/365}$) and DHAN ($I_{379/356}$). Samples were
156 included regardless of DBP type (TTHM and DHAN only) or source water and an
157 aggregate R^2 value of 0.91 indicates that fluorescence measurements can be used as a
158 reliable surrogate of organic precursor concentrations for TTHM and DHAN. As detailed
159 in the SI, UV_{254} was also assessed as a DBP surrogate, but lacked sensitivity at low
160 absorbance values (less than 0.05 cm^{-1}).

161 **Modeling CNT Wall Type**

162 Of the nine types of CNTs studied, two are single-walled (SWCNTs) and seven
163 are multi-walled (MWCNTs). To explore the effects of these designations, a binary
164 variable was added to the model to distinguish between SWCNTs and MWCNTs in
165 addition to their physical and chemical characteristics (Table 1). This binary variable was

166 significant in both TTHM and DHAN models and showed that DBP ratios were
167 significantly smaller in SWCNT-treated waters (i.e., SWCNTs adsorbed more TTHM
168 and DHAN precursors). Also, controlling for the new binary variable, CPV had negative,
169 significant effects on DBP ratio for DHAN in general (n = 36) and for TTHM in WS-EFF
170 only (n = 18). However, without more observations of SWCNT types and/or greater
171 chemical and physical detail to distinguish between single- and multi-walled CNTs, this
172 study does not focus on the general difference in CNT wall type and its relationship to
173 other variables.

174 **Removal of PARAFAC Components**

175 The maxima locations of PARAFAC Components 1 and 3 in BL-RAW (Figures
176 S5A and S5C) and WS-EFF (Figures S6A and S6C) corresponded to locations previously
177 characterized as humic- and fulvic-like fluorophores.[18] Similarly, the maxima locations of
178 Component 2 corresponded to protein-like fluorophores for BL-RAW (Figure S5B) and
179 WS-EFF (Figure S6B).[19] Component 4 in the BL-RAW model was considered negligible
180 due to its location at maximum emission wavelengths and its low F_{MAX} values, which
181 were insensitive to treatment. To gain further insight into the DBP precursors represented
182 by each PARAFAC component and their removal by the nine types of CNTs, mean
183 percent removals were calculated for each component (Table S6) based on F_{MAX} values
184 for BL-RAW and WS-EFF (Table S5).

185 Using all nine possible combinations of triplicate samples for both raw and treated
186 waters for a given CNT type, a conservatively large range of percent removal values were
187 determined and used to calculate mean removals and 95% confidence intervals using the
188 t-distribution (Table S5) due to small sample estimates of standard deviation. Removal of

189 Components 1, 2 and 3 in WS-EFF by the CNTs all show similar trends in CNT
190 performance to those observed for the removal of total THM formation potential
191 (TTHMFP) and dihaloacetonitrile formation potential (DHANFP) (Figure S7A and S7B).
192 Additionally, removal of Components 1 and 3 show strong correlations to DBPFP in BL-
193 RAW (Figure S7D and S7E). Weak correlations were observed for total *N*-nitrosamine
194 (TONO) formation potential removal (Figure S7C) and Components 2 and 4 in BL-
195 RAW. For all nine CNT types in WS-EFF, Component 2 (protein-like fluorophores) had
196 the highest mean percent removal (32-80%) of the three components. For six CNT types
197 in BL-RAW, negative mean percent removals were calculated for Component 2, which
198 was attibuted to a combination of low concentrations of protein-like compounds in BL-
199 RAW source water and interferences of humic- and fulvic-like fluorophores skewing the
200 magnitude of the fluorescent response, similar to the findings of others.[20] Additionally,
201 the samples with negative mean percent removals also have relatively large 95%
202 confidence intervals (12-339%). These observations illustrated the need for further
203 investigation into the independence of individual PARAFAC components.

204 **PARAFAC Component Correlations**

205 Linear associations between PARAFAC components were tested for data sets
206 incorporating samples treated with both low and high doses of CNTs. Correlations may
207 be considered "weak" if $R < 0.5$, "strong" if $R > 0.8$, and "moderate" otherwise.[21] As
208 shown in Table S7 for the BL-RAW samples, the correlation is strong between
209 Components 1 and 3 and moderate between Component 1 and Components 2 and 4. In
210 constrast, correlations among Components 2, 3, and 4 are weak with R values between
211 0.43-0.49. For the WS-EFF samples, all correlations were strong between the three

components, with R values of 0.85, 0.94, and 0.97. As such, even if protein-like fluorophore groups were the predominant precursors of TONO, the influence of humic- and fulvic-like fluorophores would obscure this finding and produce poor correlations such as those observed in Figure S7C.

UV_{254} as a DBP Precursor Surrogate

Performing selected linear comparisons between single dependent variables and DBPFP revealed an interesting relationship between UV_{254} and TTHMFP (Figure S9A) and DHANFP (Figure S9B). While strong linear correlations existed between UV_{254} for the WS-EFF samples (TTHMFP, $R^2 = 0.74$ and DHANFP, $R^2 = 0.78$), those for BL-RAW samples had R^2 values less than 0.01, indicating the sensitivity of the absorbance scans were insufficient for characterization of TTHM and DHAN precursors. The sensitivity of UV_{254} measurements could possibly be improved by utilizing a 5 cm pathlength cuvette, instead of the 1-cm cuvette used in this study. However, fluorescence measurements utilize a much smaller pathlength of 0.5 mm while still maintaining a comparatively high sensitivity. This in addition to its usefulness across multiple water types (Figure S4) indicates fluorescence is a more robust DBP precursor surrogate than UV_{254}.

References

1. R. M. Cory, M. P. Miller, D. M. McKnight, J. J. Guerard and P. L. Miller, *Limnol. Oceanogr. Meth.*, 2010, **8**, 67-78.
2. D. M. McKnight, E. W. Boyer, P. K. Westerhoff, P. T. Doran, T. Kulbe and D. T. Andersen, *Limnology and Oceanography*, 2001, **46**, 38-48.
3. R. G. Zepp, W. M. Sheldon and M. A. Moran, *Marine Chemistry*, 2004, **89**, 15-36.
4. T. D. Do, J. R. Chimka and J. L. Fairey, *Environ. Sci. Technol.*, 2015, **49**, 9858-9865.
5. C. M. Andersen and R. Bro, *Journal of Chemometrics*, 2003, **17**, 200-215.
6. I. Kristiana, A. Lethorn, C. Joll and A. Heitz, *Water Res.*, 2014, **59**, 90-98.
7. H. Yan Yan and E. M. Terentjev, *Polymers*, 2012, **4**, 275-295.
8. H. Ago, T. Kugler, F. Cacialli, W. R. Salaneck, M. S. P. Shaffer, A. H. Windle and R. H. Friend, *J. Phys. Chem. B*, 1999, **103**, 8116-8121.
9. M. R. McPhail, J. A. Sells, Z. He and C. C. Chusuei, *J. Phys. Chem. C*, 2009, **113**, 14102-14109.
10. Z. Zhang, L. Pfefferle and G. L. Haller, *Chinese Journal of Catalysis*, 2014, **35**, 856-863.
11. T. I. T. Okpalugo, P. Papakonstantinou, H. Murphy, J. McLaughlin and N. M. D. Brown, *Carbon*, 2005, **43**, 153-161.
12. H. Wang, A. Zhou, F. Peng, H. Yu and J. Yang, *Journal of Colloid and Interface Science*, 2007, **316**, 277-283.
13. N. I. Kovtyukhova, T. E. Mallouk, L. Pan and E. C. Dickey, *Journal of the American Chemical Society*, 2003, **125**, 9761-9769.

14. T. Ramanathan, F. T. Fisher, R. S. Ruoff and L. C. Brinson, *Chemistry of Materials*, 2005, **17**, 1290-1295.

15. B. Singh, Y. Fang, B. C. C. Cowie and L. Thomsen, *Organic Geochemistry*, 2014, **77**, 1-10.

16. S. Kundu, W. Xia, W. Busser, M. Becker, D. A. Schmidt, M. Havenith and M. Muhler, *Physical Chemistry Chemical Physics*, 2010, **12**, 4351-4359.

17. S. S. Shapiro and M. B. Wilk, *Biometrika*, 1965, **52**, 591-611.

18. A. D. Pifer and J. L. Fairey, *Environmental Engineering Science*, 2014, **31**, 117-126.

19. N. Hudson, A. Baker and D. Reynolds, *River Research and Applications*, 2007, **23**, 631-649.

20. L. M. Mayer, L. L. Schick and T. C. Loder, *Marine Chemistry*, 1999, **64**, 171-179.

21. J. L. Devore, *Probability and statistics for engineering and the sciences*, Brooks/Cole, Thomson Learning, Belmont, CA, 6 edn., 2004.

Table S1. Raw Water Characteristics

Water Type	**BL-RAW[1]**	**WS-EFF[2]**
pH	7.82	7.93
DOC[3] ($mg \cdot L^{-1}$)	2.33	5.98
UV_{254} (cm^{-1})	0.034	0.096
$I_{345/425}$ (QSE)[4]	5.16	14.25
Specific Conductivity ($\mu S \cdot cm^{-1}$)	155	535
Fluoride ($mg \cdot L^{-1}$)	0.11	0.47
Chloride ($mg \cdot L^{-1}$)	4.1	47.9
Bromide ($mg \cdot L^{-1}$)	0.11	0.16
Nitrate ($mg \cdot L^{-1}$)	1.3	23.9
Phosphate ($mg \cdot L^{-1}$)	ND[5]	0.29
Sulfate ($mg \cdot L^{-1}$)	8.0	47.2
Nitrite ($mg \cdot L^{-1}$)	ND	ND

[1]Raw intake water from Beaver Lake collected on July 7, 2014
[2]Effluent from the West Side Wastewater Treatment Plant collected on June 3, 2014
[3]Dissolved Organic Carbon
[4]Average fluorescence intensity at excitation and emission wavelengths of 325 nm and 425 nm respectively
[5]Not detected

Table S2. Manufacturer-specified properties of the selected carbon nanotubes.

CNT[1] Number	CNT Type	Supplier Description	Diameter (nm)	Length (mm)	S_{BET}[2] (m^2 g^{-1})	Supplier
1	SW[3]	SWNTs (90%, regular length)	1-2	5-30	300-380	NAM, Inc. [4]
2		SW-DW CNTs 60	0.8-1.6	5-30	407	Cheap Tubes, Inc.
3	MW[5]	C-Grade MWNTs	1-3	80-150	NA[6]	NanoTechLabs, Inc.
4		MW CNTs 8 nm	2-5	10-30	500	Cheap Tubes, Inc.
5		MW CNTs 20-30 nm	5-10	10-30	110	Cheap Tubes, Inc.
6		95%, OD/ID: <10/2-7 nm	2-7	5-15	40-600	NAM, Inc.
7		95%, OD/ID: 30-50/5-15 nm	5-15	10-20	90-120	NAM, Inc.
8		PD30L5-20	15-45	5-20	200-400	NanoLab, Inc.
9		PD30L1-5	15-45	1-5	200-400	NanoLab, Inc.

[1]Carbon nanotube
[2]Supplier provided specific surface area from nitrogen adsorption isotherms using the Brunauer-Emmett-Teller (BET) model
[3]Single-walled
[4]Nanostructured & Amorphous Materials, Inc.
[5]Multi-walled
[6]Not Available

279

280 **Table S3.** Preliminary DBPFP Removal Testing

CNT Dose (mg L^{-1})[1]	Water Type[2]	Average TTHMFP[3] Removal (%)	Average DHANFP[4] Removal (%)
0	BL-RAW	-	-
5	BL-RAW	14	-
50	BL-RAW	51	-
520	BL-RAW	98	-
0	BL-RAW	-	-
5	BL-RAW	26	37
50	BL-RAW	71	94
0	WS-EFF	-	-
5	WS-EFF	11	20
50	WS-EFF	67	96

[1]Single-walled CNTs were used in all dosed samples
[2]Beaver Lake raw water (BL-RAW) was collected on August 15, 2013 for first set of samples and April 5, 2014 for the second set. West Side WWTP effluent (WS-EFF) was collected on April 9, 2014.
[3]Average total trihalomethane formation potential based on duplicate samples
[4]Average dichloroacetonitrile formation potential based on duplicate samples

281

Table S4. Chlorine Residuals following filtration in batch studies

CNT Type	CNT Dose ($mg \cdot L^{-1}$)	Average Chlorine Residual ($mg \cdot L^{-1}$)	
		BL-RAW	**WS-EFF**
Blank	0	9.29	9.26
1	25	11.30	10.27
	50	11.47	10.18
2	25	13.83	11.32
	50	14.47	11.23
3	25	14.63	12.77
	50	14.90	12.31
4	25	14.09	12.03
	50	14.85	12.37
5	25	14.35	12.40
	50	14.22	10.72
6	25	15.30	12.65
	50	15.23	13.50
7	25	13.19	12.43
	50	14.00	13.18
8	25	14.76	11.20
	50	15.37	10.49
9	25	11.94	11.48
	50	13.80	10.80

286 **Table S5.** Fluorescence maximum (F_{MAX}) values

CNT Type	CNT Dose (mg L^{-1})	Water Type						
		BL-RAW				WS-EFF		
		C1	C2	C3	C4	C1	C2	C3
Blank	0	9.7	5.1	3.0	1.8	17.1	10.1	9.5
		9.9	4.9	3.1	1.8	18.2	11.0	12.5
		9.9	4.3	3.0	1.8	18.0	10.9	12.1
1	25	4.2	1.9	1.1	1.5	8.1	3.5	4.8
		4.2	1.9	1.2	1.6	8.1	3.4	5.0
		4.3	2.0	1.2	1.4	8.4	3.6	5.8
	50	3.2	1.5	0.9	1.6	5.6	2.2	4.0
		3.2	1.5	0.9	1.3	5.6	2.2	4.4
		3.6	1.9	0.9	1.6	5.4	2.1	5.0
2	25	4.7	2.1	1.6	1.5	7.4	4.0	4.0
		4.9	2.1	1.6	1.5	7.5	4.1	4.2
		4.6	2.2	1.5	1.4	7.5	4.1	4.4
	50	3.2	1.6	1.0	1.3	4.4	2.3	2.6
		1.8	1.4	1.0	1.7	4.4	2.3	2.6
		4.0	3.2	1.6	1.7	4.5	2.4	2.9
3	25	8.0	6.5	2.3	2.4	13.1	6.4	9.4
		8.2	8.1	2.2	1.8	13.0	6.2	9.2
		7.8	4.5	2.2	1.8	13.6	6.5	10.1
	50	7.2	6.6	2.1	2.7	10.1	4.2	7.9
		5.2	2.0	1.6	1.6	9.9	4.0	6.8
		7.2	4.0	1.9	1.8	10.0	4.1	7.6
4	25	5.5	3.9	1.6	1.8	8.9	3.5	6.3
		5.6	6.0	1.6	2.0	7.8	3.1	4.7
		5.5	3.8	1.6	1.9	8.3	3.4	6.1
	50	4.2	3.2	1.2	1.6	5.5	2.1	3.9
		4.0	3.5	1.3	1.8	5.6	2.2	4.3
		4.1	3.3	1.2	1.7	5.7	2.2	4.4
5	25	6.1	6.9	1.9	1.8	10.9	4.8	8.2
		6.6	6.9	2.0	1.7	10.8	4.8	7.7
		6.7	9.9	2.0	1.8	11.1	5.0	9.1
	50	4.7	2.8	1.4	1.6	7.8	3.1	6.3
		5.5	4.9	1.7	1.8	7.9	3.2	6.2
		5.0	3.5	1.4	1.8	7.5	3.0	5.1
6	25	6.8	15.3	1.9	1.9	9.2	3.8	6.7
		6.7	13.3	1.9	1.9	9.2	3.9	6.4
		7.4	7.7	2.1	2.2	9.5	3.9	6.5

287
288

289 **Table S5 Continued.**

CNT Type	CNT Dose (mg L^{-1})	Water Type						
		BL-RAW				WS-EFF		
		C1	C2	C3	C4	C1	C2	C3
6	50	4.9	3.0	1.3	1.8	6.7	2.5	5.3
		-	-	-	-	6.2	2.4	4.2
		5.6	14.3	1.5	1.8	6.6	2.5	5.3
7	25	9.5	10.5	2.7	2.0	14.2	7.1	10.7
		10.2	11.1	2.9	2.0	14.1	7.2	10.7
		7.9	5.2	2.3	1.9	14.1	7.3	10.9
	50	7.8	17.6	2.1	2.0	11.6	5.1	10.5
		6.7	9.8	2.0	1.9	11.6	5.2	9.0
		8.9	10.8	2.2	2.3	11.7	5.3	9.2
8	25	-	-	-	-	8.9	3.4	7.1
		6.5	7.3	1.7	2.1	9.2	3.6	7.5
		6.1	10.7	1.7	1.7	10.1	3.9	8.4
	50	4.7	8.0	1.5	1.7	6.7	2.5	5.8
		3.7	3.4	1.2	1.4	6.6	2.3	7.4
		4.5	10.0	1.3	1.6	6.5	2.4	5.3
9	25	5.7	8.6	1.5	1.7	9.7	4.0	7.4
		5.5	6.2	1.6	1.7	9.4	3.9	7.1
		5.6	6.8	1.8	2.3	9.5	3.8	7.8
	50	4.7	8.5	1.4	1.7	6.5	2.4	4.8
		4.1	7.5	1.3	2.1	6.6	2.4	5.0
		4.5	4.1	1.4	1.6	6.6	2.5	5.2

290
291

Table S6. Mean percent removal of each PARAFAC component

Water Type	CNT Type	Dose = 25 mg/L CNTs			
		C1[1]	C2	C3	C4
BL-RAW	1	57 ± 2.5[2]	59 ± 11	62 ± 2.3	16 ± 16
	2	52 ± 5.0	55 ± 14	48 ± 6.3	19 ± 7.8
	3	19 ± 8.4	-37 ± 123	27 ± 6.1	-11 ± 48
	4	44 ± 2.3	2 ± 89	47 ± 2.6	-7 ± 12
	5	34 ± 10	-70 ± 129	36 ± 7.2	2 ± 5.6
	6	29 ± 12	-160 ± 252	35 ± 13	-11 ± 30
	7	6 ± 33	-92 ± 200	12 ± 27	-9 ± 14
	8	36 ± 7.1	-93 ± 129	44 ± 2.6	-5 ± 28
	9	43 ± 4.0	-53 ± 102	46 ± 10	-5 ± 55
WS-EFF	1	54 ± 6.2	67 ± 5.4	53 ± 30	-[3]
	2	58 ± 4.1	62 ± 5.5	62 ± 18	-
	3	25 ± 10.9	40 ± 11	14 ± 43	-
	4	53 ± 11.3	69 ± 7.5	49 ± 35	-
	5	38 ± 7.6	54 ± 8.1	25 ± 43	-
	6	47 ± 6.6	64 ± 5.5	42 ± 25	-
	7	20 ± 7.5	32 ± 10	4 ± 40	-
	8	47 ± 13	66 ± 10	31 ± 42	-
	9	46 ± 6.5	63 ± 6.1	33 ± 33	-

[1]Components 1-4 represented as C1-C4
[2]95% confidence intervals calculated from maximum range of possible removal values
[3]Model for WS-EFF were only validated with a maximum of three components

Table S6 Continued.

Water Type	CNT Type	Dose = 50 mg/L CNTs			
		C1	C2	C3	C4
BL-RAW	1	66 ± 7.5	65 ± 18	70 ± 1.2	15 ± 25
	2	69 ± 30	55 ± 62	60 ± 27	10 ± 32
	3	34 ± 31	8 ± 145	39 ± 21	-12 ± 86
	4	58 ± 3.5	29 ± 21	59 ± 4.9	4 ± 21
	5	49 ± 12	20 ± 76	51 ± 12	2 ± 18
	6	47 ± 11	-89 ± 339	54 ± 9.6	1 ± 3.6
	7	21 ± 31	-175 ± 292	31 ± 14	-16 ± 32
	8	56 ± 15	-54 ± 206	56 ± 14	13 ± 23
	9	55 ± 9.0	-44 ± 145	54 ± 8.0	1 ± 38
WS-EFF	1	69 ± 4.1	80 ± 3.5	60 ± 27	-
	2	75 ± 3.0	78 ± 3.4	75 ± 14	-
	3	44 ± 6.4	61 ± 5.9	33 ± 37	-
	4	68 ± 4.3	80 ± 3.6	62 ± 20	-
	5	56 ± 5.7	71 ± 4.9	47 ± 32	-
	6	63 ± 6.5	77 ± 4.6	56 ± 27	-
	7	34 ± 6.2	51 ± 8.2	14 ± 52	-
	8	63 ± 5.0	77 ± 4.7	44 ± 47	-
	9	63 ± 3.9	77 ± 3.4	55 ± 21	-

297 **Table S7.** Linear correlations (R) between components of BL-RAW and WS-EFF

298 PARAFAC Models

Water Type		Components		
		C1	**C2**	**C3**
BL-RAW	**C2**	0.51	-	-
	C3	0.97	0.43	-
	C4	0.54	0.47	0.49
WS-EFF	**C2**	0.97	-	-
	C3	0.94	0.85	-

299

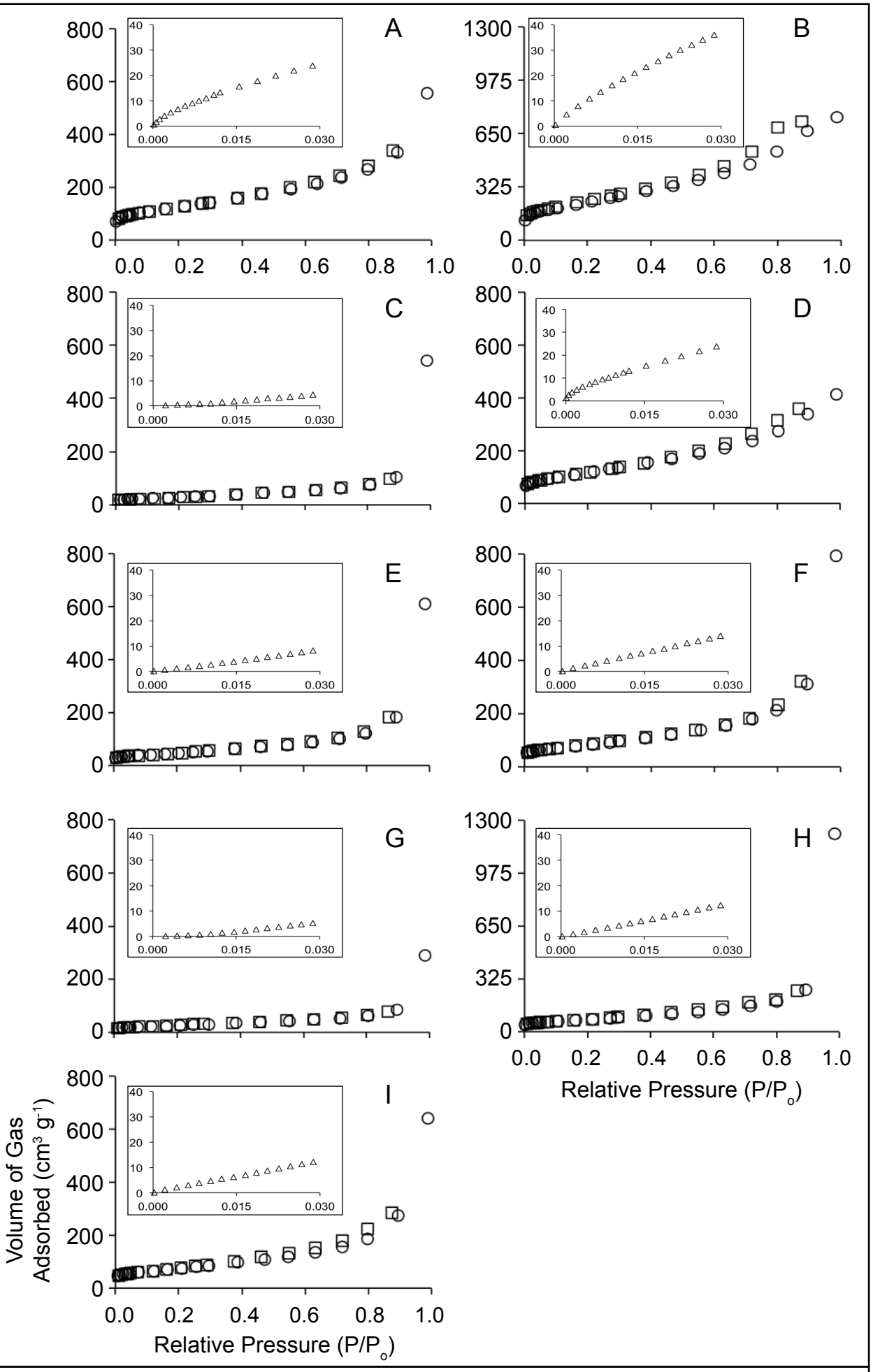

Figure S1. Gas Adsorption Isotherms for CNT Types 1-9 (Figures S1A-S1I). Nitrogen gas adsorption (○) and desorption (□) loops are accompanied by inset carbon dioxide gas adsorption (△) loops. Units are constant for all isotherms.

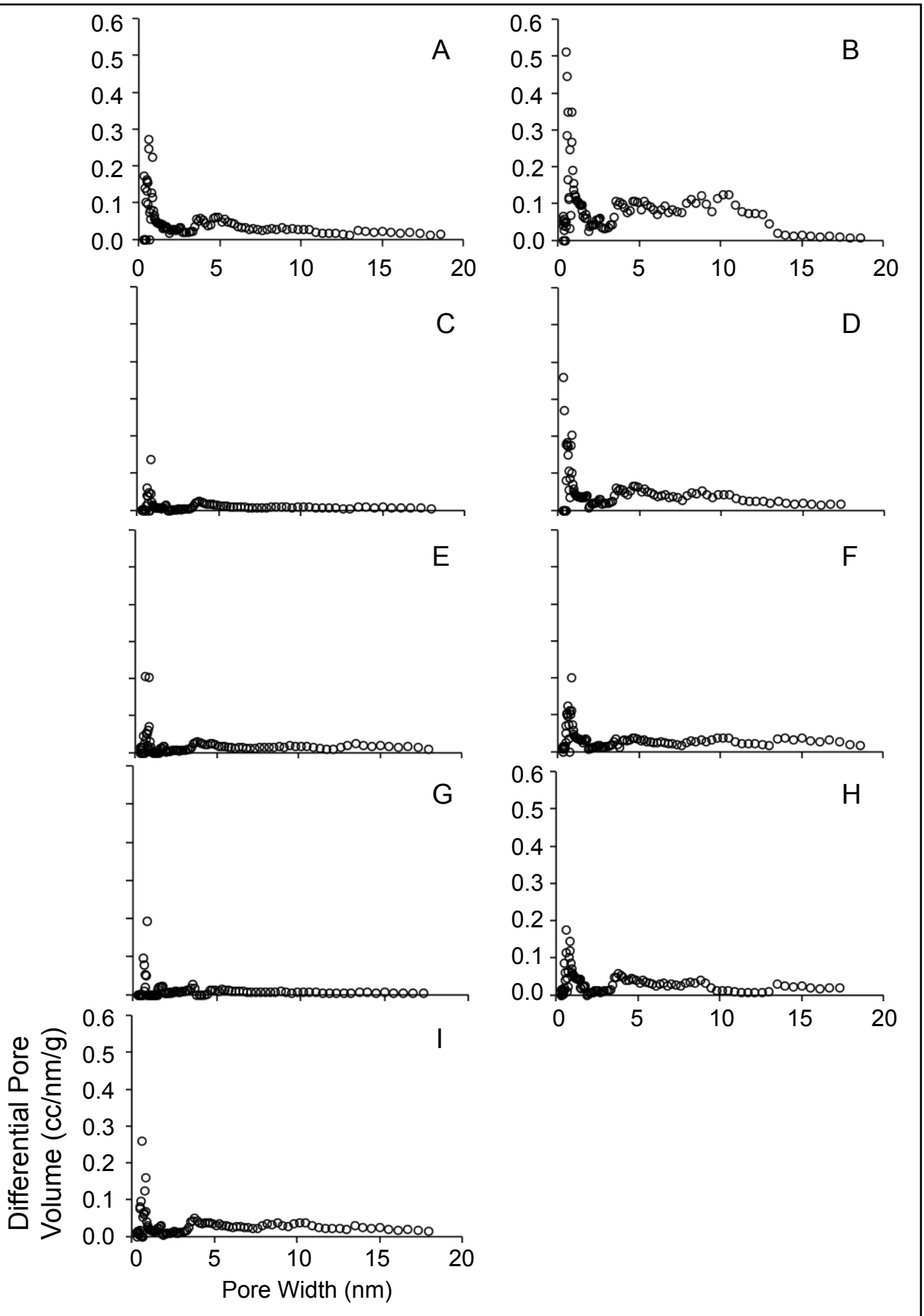

Figure S2. Pore volume distributions for CNT Types 1-9 (Figures S2A-S2I), all with identical scales

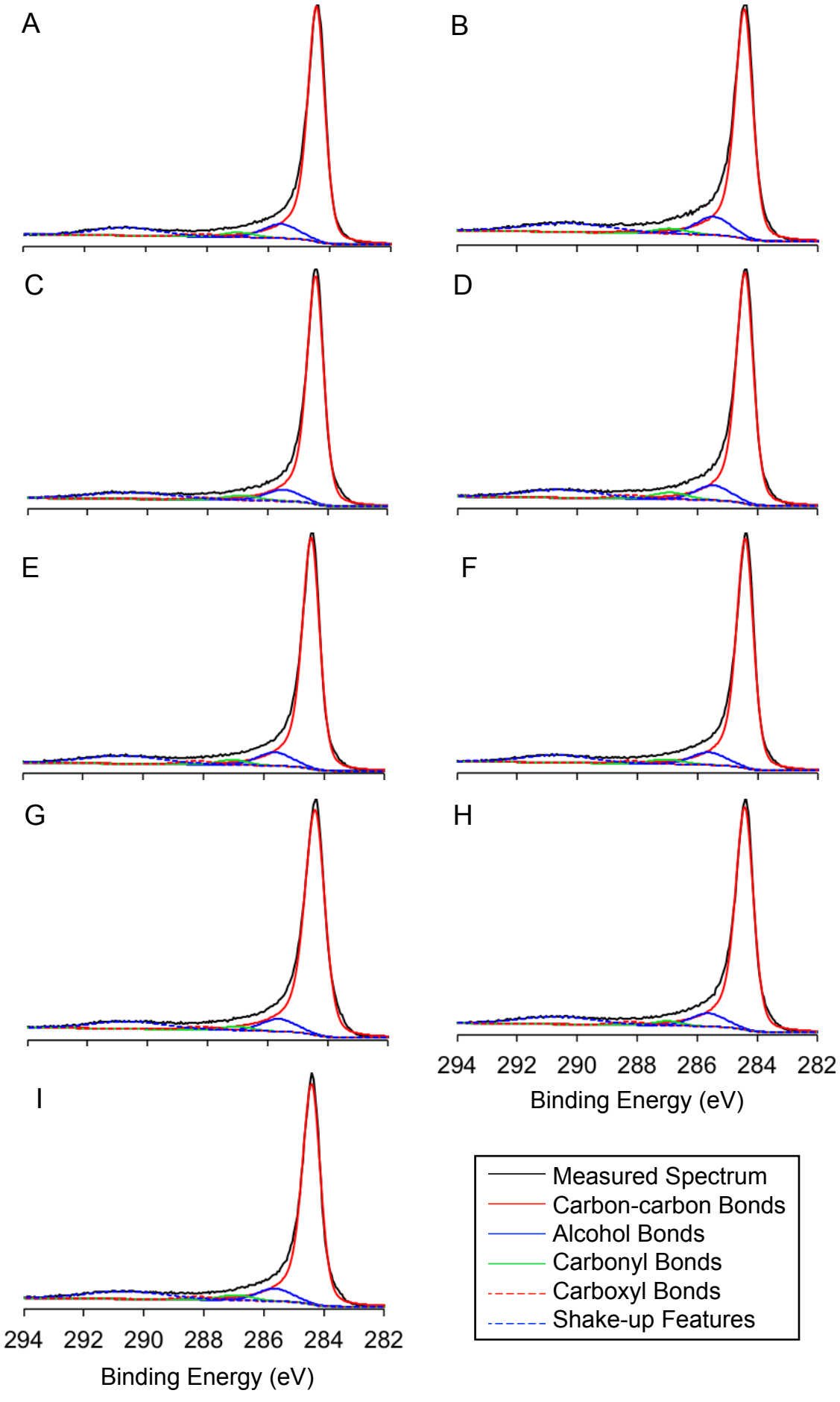

Figure S3. Deconvolutions of Carbon Spectra from XPS Measurements for CNT Types 1-9 (Figures S3A-S3I)

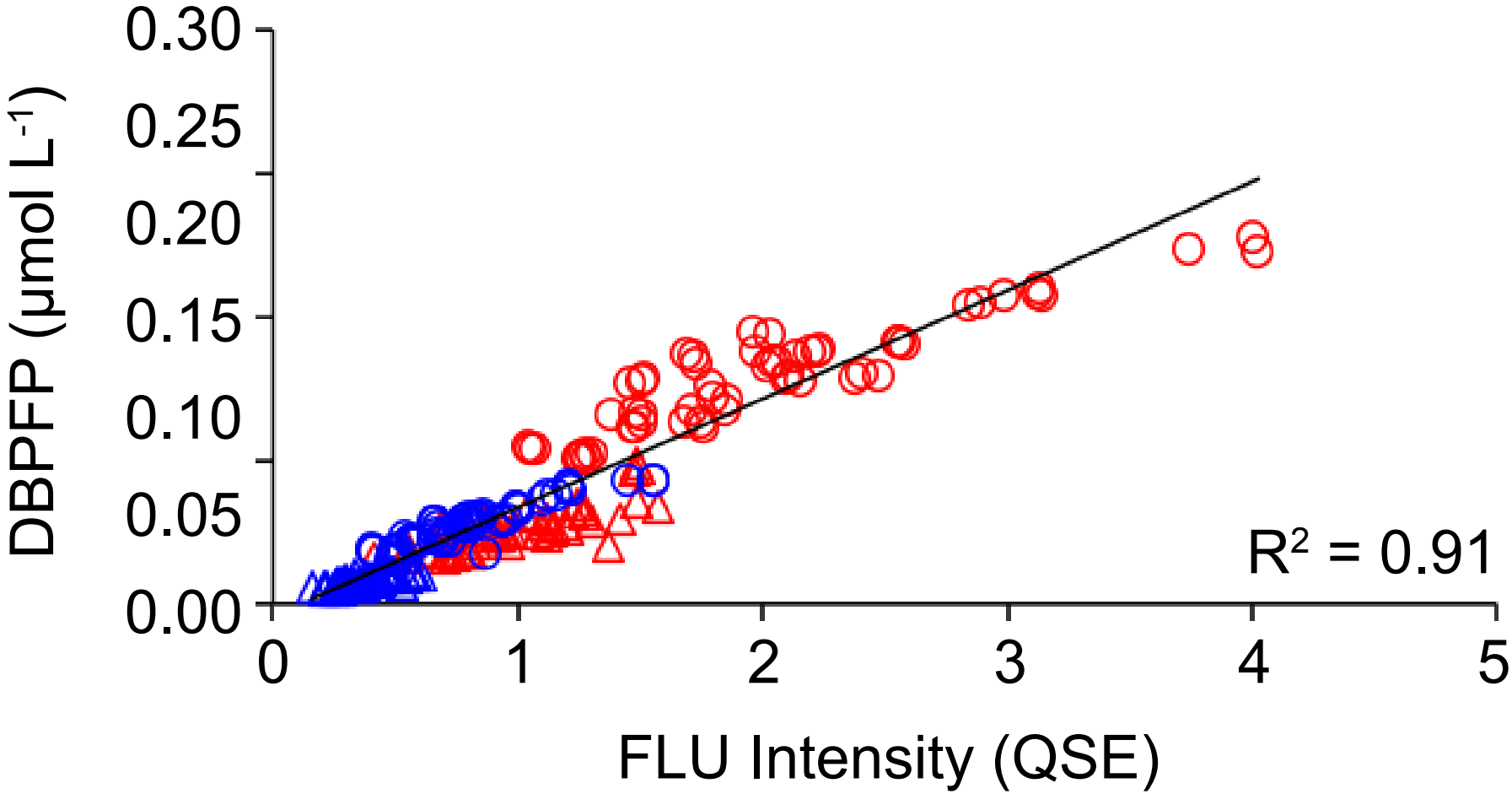

Figure S4. Linear regression of fluorescence at R_{MAX}^2 excitation-emission wavelength pairs against TTHMFP in BL-RAW (△) and WS-EFF (○) and DHANFP in BL-RAW (△) and WS-EFF (○).

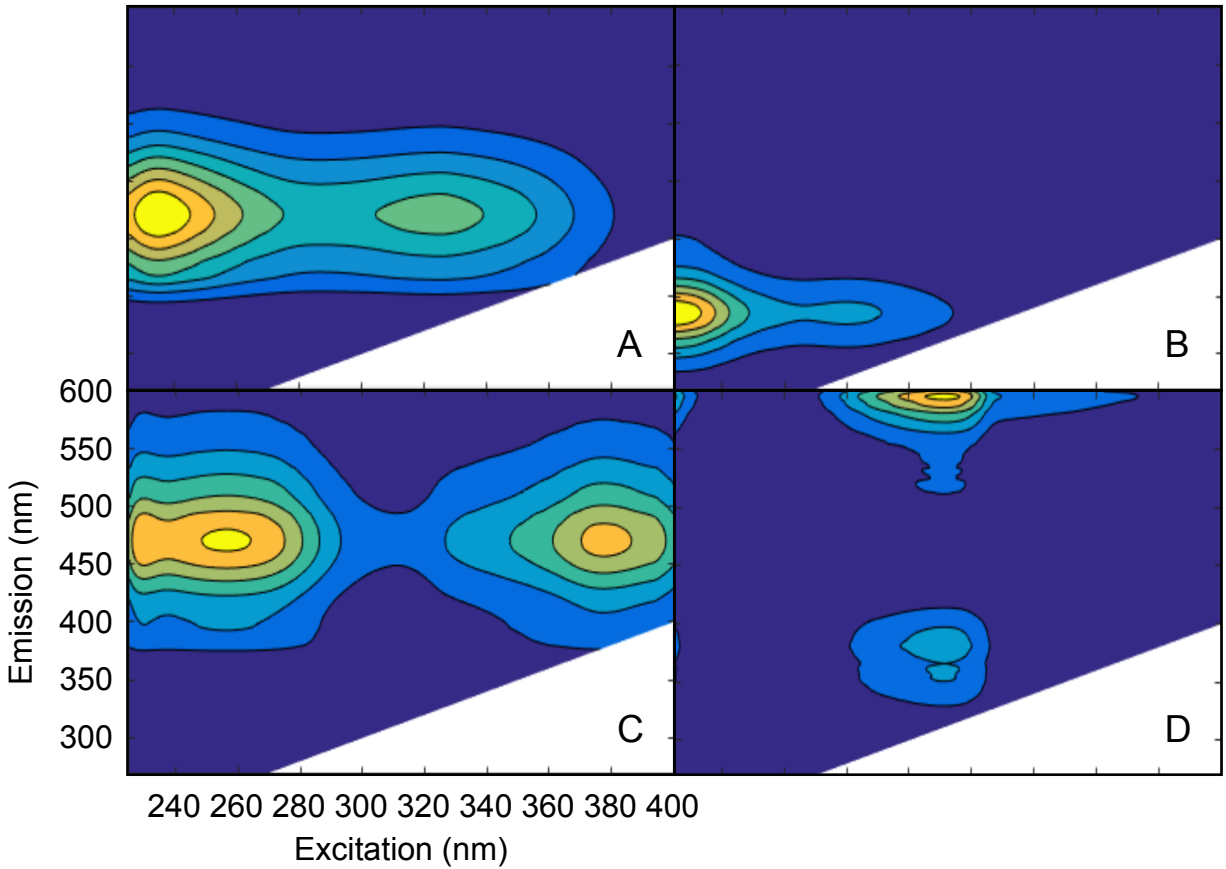

Figure S5. PARAFAC Component EEMs for Beaver Lake Raw Water. A) Component 1, B) Component 2 and D) Component 4 utilize the axes specified in C) Component 3.

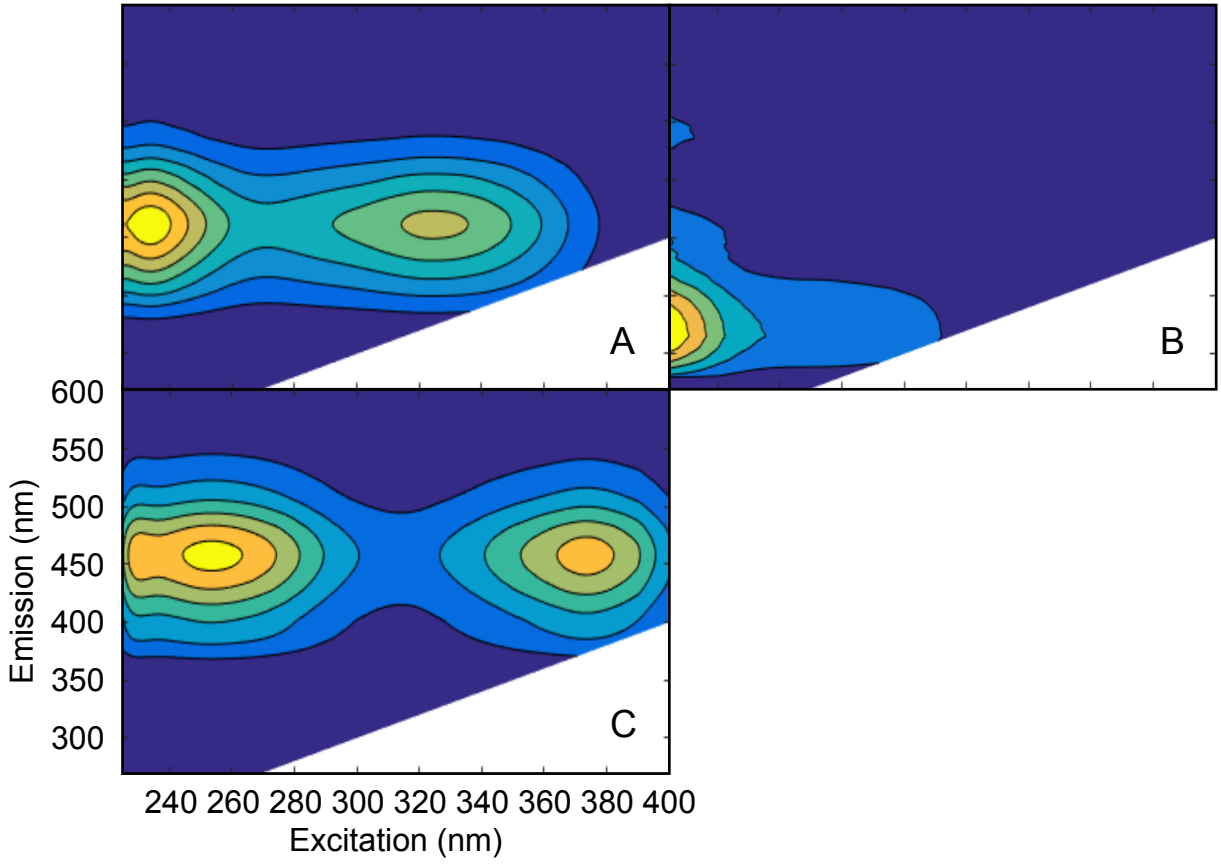

Figure S6. PARAFAC Component EEMs for West Side WWTP Effluent. A) Component 1 and B) Component 2 utilize the axes specified in C) Component 3.

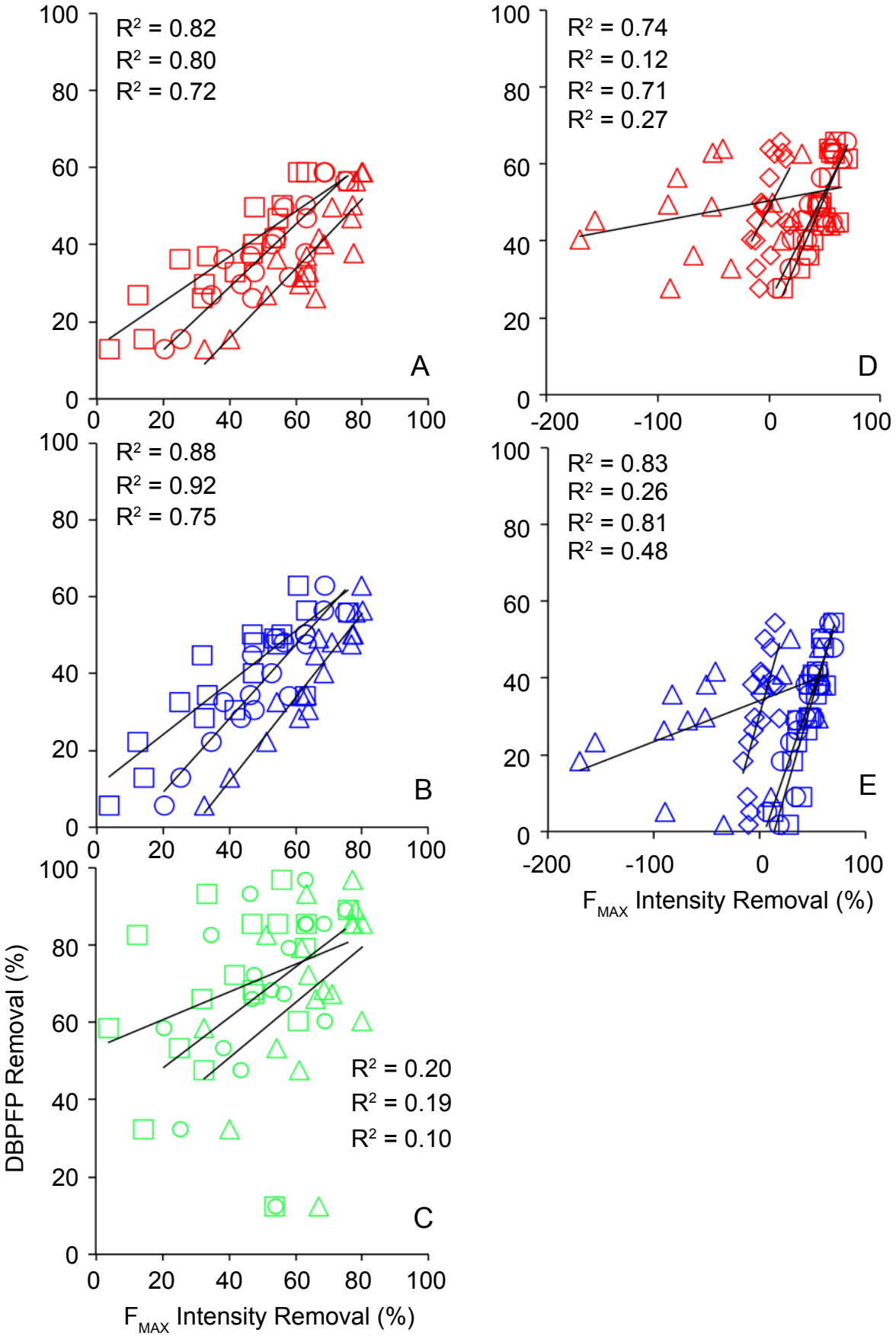

Figure S7. Linear regressions of DBPFP percent removal against percent removal of F_{MAX} of PARAFAC Components 1 (○), 2 (△), 3 (□), and 4 (◇) for TTHMFP, DHANFP, and TONOFP (Figures S8A-S8C) in WS-EFF and TTHMFP and DHANFP (Figures S8D and S8E) in BL-RAW. R^2 values appear according to numerical Component order.

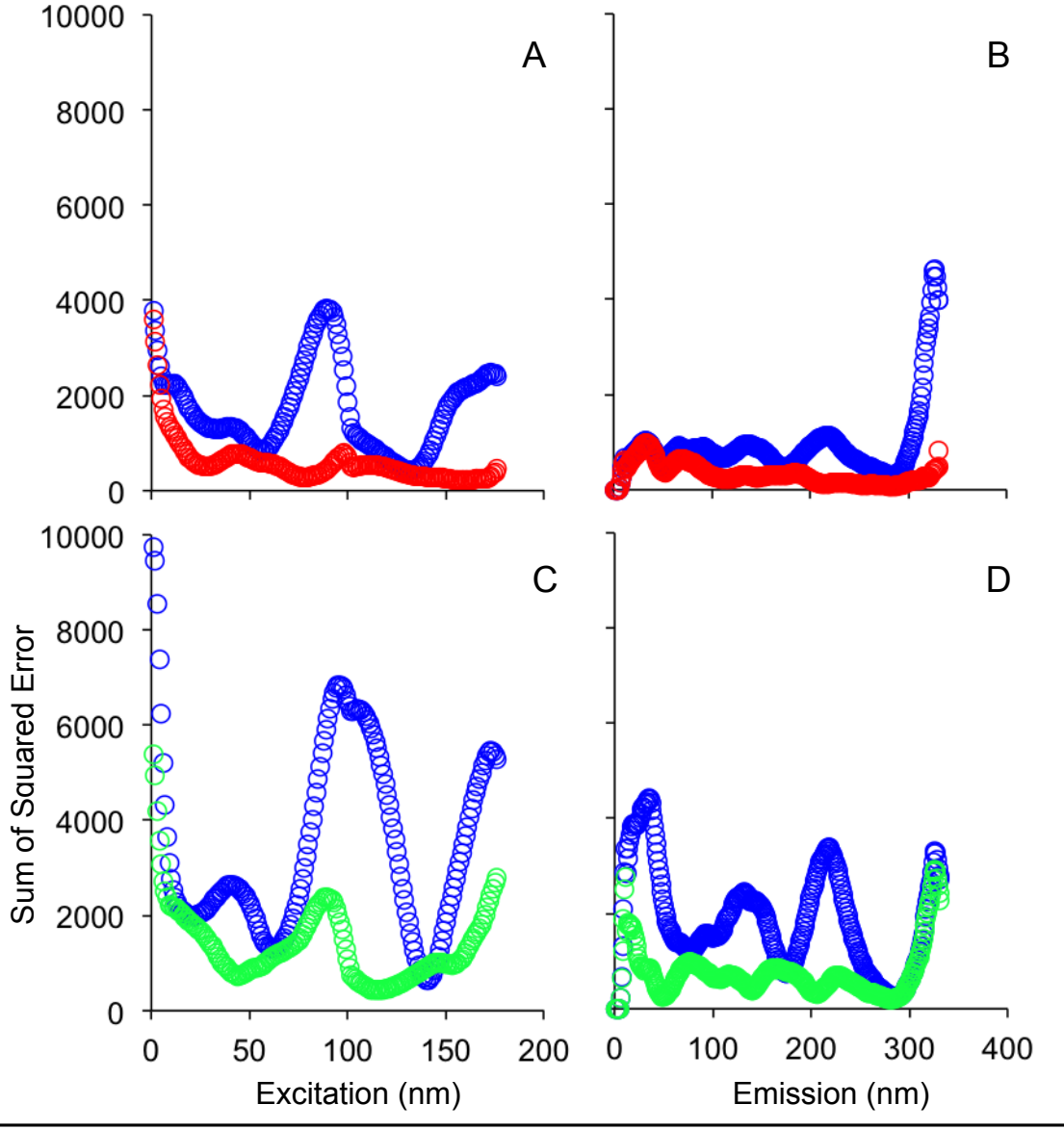

Figure S8. Sum of squared errors for excitation and emission wavelengths based on PARAFAC models with varying quantities of components. Two component (○) and 4 component (○) models were validated for BL-RAW (Figure S9A and S9B). Two component and three component (○) models were validated for WS-EFF (Figure S9C and S9D).

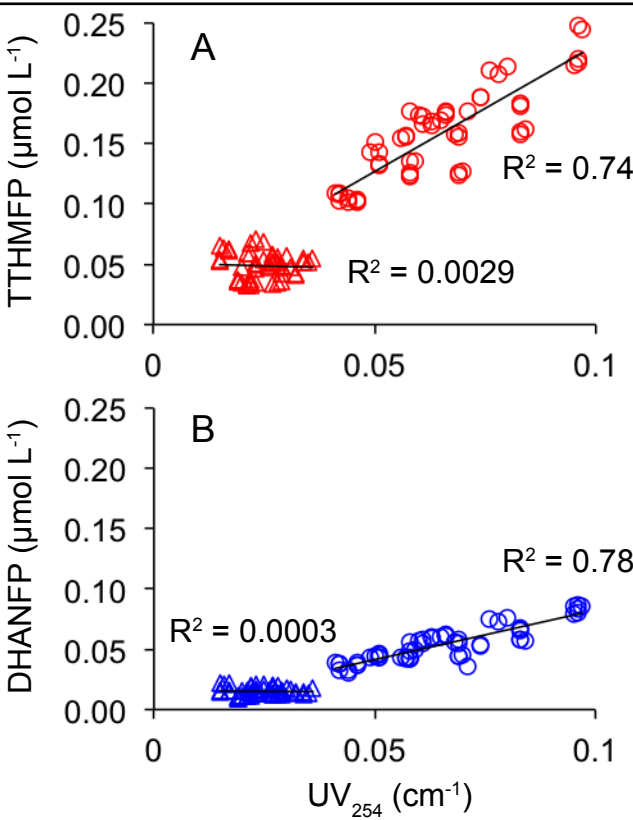

Figure S9. Linear regression of TTHMFP in BL-RAW (○) and WS-EFF (△) (Figure S10A) and DHANFP in BL-RAW (○) and WS-EFF (△) (Figure S10B).